Journal of General Virology (2010), **91**, 1728–1736 **DOI** 10.1099/vir.0.019323-0

Role of heat-shock protein 90 in hepatitis E virus capsid trafficking

Zi-Zheng Zheng, Ji Miao, Min Zhao, Ming Tang, Anthony E. T. Yeo, Hai Yu, Jun Zhang and Ning-Shao Xia

National Institute of Diagnostics and Vaccine Development in Infectious Diseases, School of Life Sciences, Xiamen University, Xiamen 361005, PR China

Correspondence
Ning-Shao Xia
zhengzizheng@xmu.edu.cn

p239 is a virus-like particle constituted from hepatitis E virus (HEV) recombinant proteins. It can be used as a surrogate for HEV and as an investigative tool to study cellular interactions because of its ability to adsorb to and penetrate HepG2 cellular membranes. Our objective was to use p239 to define the role of HEV capsid proteins during the early stages of infection. Pull-down and MALDI-TOF MS experiments identified three host-cell proteins, Grp 78/Bip, α-tubulin and heat-shock protein 90 (HSP90), and the latter was investigated further. Antibodies to p239 alone or HSP90 alone could detect p239 or HSP90, suggesting the formation of a complex between p239 and HSP90. In the HepG2 cell, geldanamycin (GA), an HSP90-specific inhibitor, blocked intracellular transportation of p239, but had no effect on the binding and cellular entry of p239, suggesting that HSP90 was important for HEV capsid intracellular transportation. RT-PCR results showed that the efficiency of wild-type HEV infection was inhibited significantly by GA treatment, suggesting the importance of HSP90 in virus infectivity. It was concluded that HSP90 plays a crucial role in the intracellular transportation of viral capsids in the early stage of HEV infection.

Received 17 December 2009
Accepted 8 March 2010

INTRODUCTION

Hepatitis E virus (HEV) is a small, non-enveloped, single positive-stranded RNA virus with an icosahedral capsid of approximately 30 nm diameter (Bradley *et al.*, 1988). The viral genome of 7.5 kb is organized as three open reading frames (ORFs). ORF1, mapping to the 5′ terminus, encodes a non-structural protein that probably undergoes post-translational cleavage into multiple non-structural proteins required for virus replication. ORF2, mapping to the 3′ terminus, encodes the exclusive capsid protein, which contains a signal sequence at its N terminus. The N-terminal region of the capsid protein is postulated to interact with the negatively charged genomic RNA, while the C-terminal region of the protein contains several antigenic sites, including a neutralization epitope located from residues 452 to 617 (Meng *et al.*, 2001). The determination of the three-dimensional crystal structure of HEV virus-like particles (VLPs) in recent studies showed that the N terminus of ORF2 also plays a key role in the assembly of the HEV particle (Guu *et al.*, 2009; Yamashita *et al.*, 2009). ORF3 overlaps extensively with ORF2, encoding a small immunogenic protein of 123 aa, recently suggested to be only a 114 aa (Graff *et al.*, 2006; Huang *et al.*, 2007) phosphoprotein that is currently of unconfirmed significance.

A bacterially expressed, truncated viral structural peptide, p239 (ORF2, aa 368–606), has been found to occur as 23 nm particles in neutral solution (Li *et al.*, 2005). It migrates predominantly as a dimer in SDS-PAGE and is strongly reactive with acute and convalescent serum from hepatitis E patients (Li *et al.*, 2005). p239 inoculation has been shown to protect the rhesus monkey from infection after challenge with a dose of 10^4 genome equivalents of homologous genotype 1 or genotype 4 virus. At a higher dose of 10^7 genome equivalents, p239 protected the animals from acute hepatitis (Li *et al.*, 2005). Recently, two conformational-dependent neutralizing epitopes, 8C11 and 8H3, were identified using p239 (Zhang *et al.*, 2005). These data indicate that p239 is a good candidate for an HEV vaccine and also suggests that p239 should have a similar surface structure to native HEV particles.

Virus attachment and entry into the host are the first steps in successful infection. In HEV, these processes are largely unknown because of the lack of a reliable cell-culture system or animal model. Therefore, in order to be able to investigate further, p239 can be used as a surrogate for HEV because of its antigenicity, immunogenicity and genetic homology to HEV. He *et al.* (2008) used p239 to simulate native HEV to investigate virus attachment on hepatocytes. It has also been shown that p239 attached and entered the cells of four susceptible cell lines, HepG2 (Emerson *et al.*, 2004, 2005; Graff *et al.*, 2008), Huh7 (Emerson *et al.*, 2004, 2005; Graff *et al.*, 2008), PLC/PRF5 (Meng *et al.*, 1997; Tanaka *et al.*, 2007) and A549 (Huang *et al.*, 1995; Tanaka *et al.*, 2007), and binding was blocked by neutralizing monoclonal antibodies (mAbs). Moreover, the interaction between p239 and the host cells was

dependent on the dimeric conformation fit of p239 and the binding significantly inhibited HEV infectivity on HepG2 and Huh7 cells. The three-dimensional crystal structure of HEV VLP further demonstrates that this peptide is on the surface of the viral capsid protein, suggesting that it has an important functional role in cell entry (Guu *et al.*, 2009; Li *et al.*, 2009; Yamashita *et al.*, 2009).

In the present study, p239-interacting proteins were isolated and identified by using a pull-down assay and two-dimensional gel separation, followed by a mass spectrometry assay. Several binding candidates were identified and their virus entry-related functions were analysed.

RESULTS

Construction and characterization of p239–CBP

Calmodulin-binding peptide (CBP), a tag binding to calmodulin (CaM)–Sepharose, was fused with p239, to form p239–CBP, and characterized. p239–CBP showed a similar reactivity profile to HEV-neutralizing mAbs 8C11 and 8H3 in ELISA analysis (Fig. 1a). It also had a similar retention time on molecular sieve chromatography (Fig. 1b) with p239. Localization of p239–CBP incubated with HepG2 cells was detected by an immunofluorescence assay (Fig. 1c). p239–CBP attached to the cell membrane. Entry of p239–CBP into the hepatocyte was noted after 30 min incubation and it was localized in the cytoplasmic region. This result is consistent with a previous study (He *et al.*, 2008). Additionally, CBP did not appear to affect the structure and antigenicity of p239.

Isolation and identification of p239 proteins

Proteins that interacted with p239–CBP were isolated and separated by two-dimensional gel electrophoresis with specific protein spots marked by arrowheads (Fig. 2a). Spot 'a' was identified as heat-shock protein 90 (HSP90) and Western blotting of the eluted sample was performed using an HSP90-specific antibody. Reactive bands were observed (Fig. 2b), which supported the findings from MALDI-TOF MS analysis. p239 was detected in the immune complex precipitated by an anti-HSP90 antibody (Fig. 2c, lower panel). Additionally, an HSP90-reactive band was observed (Fig. 2c, upper panel). These results suggested an interaction between p239 and HSP90.

HSP90 showed co-localization with p239

p239 and HSP90 fluorescence signals in p239-incubated HepG2 cells were examined by time-course experiments using confocal microscopy. At 0 h, p239 was detected on the surface of cells [Fig. 3a (v)], indicating that p239 attached to the plasma membrane immediately after being added to the culture medium. By 4 h, most of the p239 was present intracellularly [Fig. 3a(viii)] and then a gradual decrease commenced (Fig. 3b). By 32 h, the fluorescent signal was hardly observed [Figs 3a(xi) and 3b]. Further, the addition of p239 resulted in a change in the intracellular distribution of HSP90, with likely co-localization of the two proteins [Fig. 3a(vi, ix and xii)].

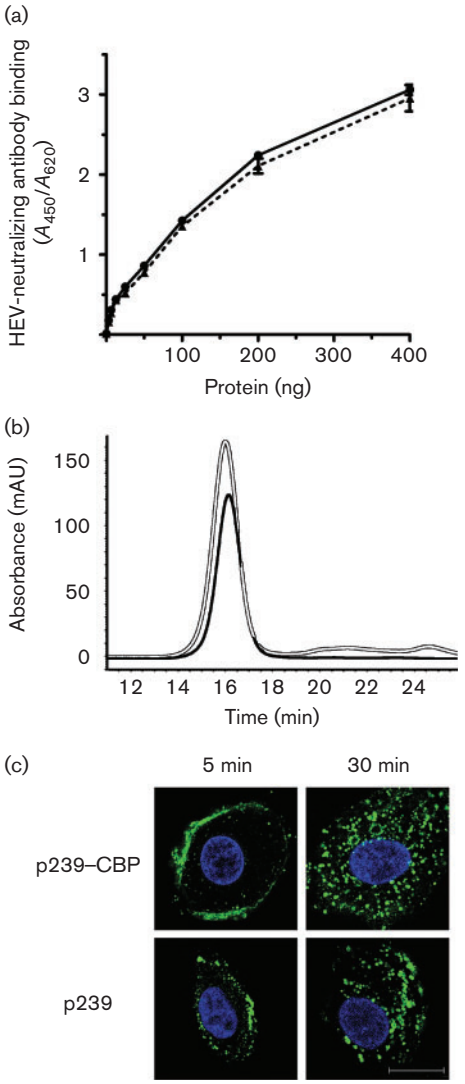

Fig. 1. Comparison between p239 and p239–CBP. (a) Reactivity of p239 (●) and p239–CBP (▲) with HEV-neutralizing antibodies 8C11 and 8H3 by two-site sandwich ELISA. (b) Retention time of p239 (black line) and p239–CBP (white line) on molecular sieve chromatography. (c) Binding and penetration of p239 and p239–CBP on HepG2 cells as shown by immunofluorescence; bar, 10 μm. The results from these experiments show that p239 and p239–CBP have similar physical and biological characteristics.

Inhibition of p239 trafficking by using an HSP90 inhibitor – geldanamycin (GA)

In contrast to cytoplasmic localization in cells without treatment [Figs 3a(i–iii) and 4c, lower panels], most p239

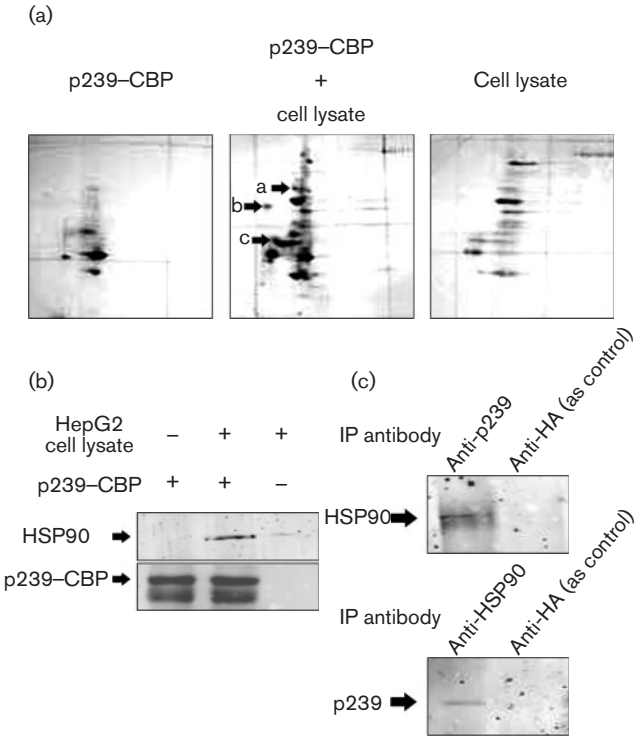

Fig. 2. Isolation and identification of HEV capsid-binding proteins. Proteins interacting with p239 were pulled down with p239–CBP-conjugated CaM–Sepharose from HepG2 cell lysate and analysed by two-dimensional electrophoresis (a) and Western blot assay (b). (a) Specific binding proteins are marked with arrows (middle panel) compared with controls (left panel, p239–CBP bound to CaM–Sepharose; right panel, proteins from cell lysate that interacted non-specifically with CaM–Sepharose). (b) The Western blot result indicates an apparent HSP90 reactivity in the p239–CBP pull-down component (middle lane), but it was not observed in controls (left lane, p239–CBP bound to CaM–Sepharose; right lane, proteins from cell lysate that interacted non-specifically with CaM–Sepharose). (c) Immunoprecipitation of p239 and HSP90 from p239-treated HepG2 cell lysate. Immune complexes were isolated with anti-p239 antibody (15B2) then immunoblotted with anti-HSP90 antibody (upper panel). Alternatively, the complexes were isolated with anti-HSP90 antibody and then immunoblotted with anti-p239 antibody (15B2, lower panel). An anti-haemagglutinin (HA) antibody was used as control. Results from both panels show specific interaction between p239 and HSP90.

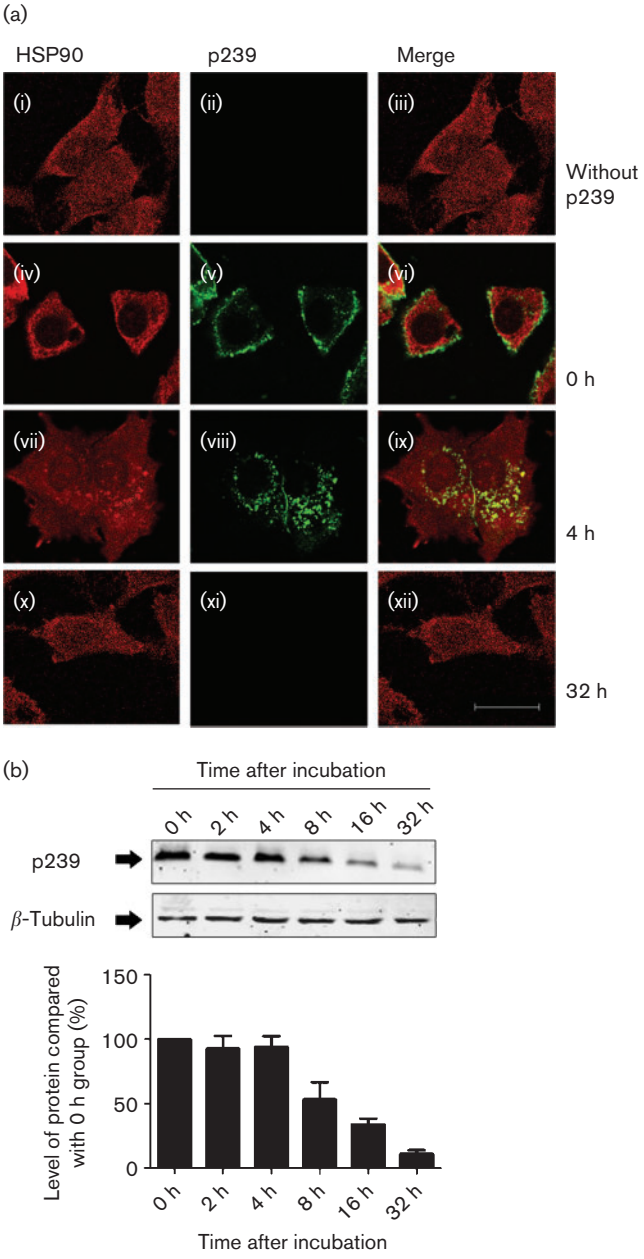

Fig. 3. Presence of p239 in HepG2 cells pre-incubated with p239 and harvested at 0, 2, 4, 8, 16 and 32 h after reincubation at 37 °C. (a) Localization of p239 and HSP90 in the cells. According to the localization of p239, the process was divided into three stages and showed: attachment (0 h, panels iv–vi), intracellular localization (4 h, panels vii–ix) and degradation (32 h, panels x–xii). Localization of HSP90 in native HepG2 cells without adding p239 is shown in panels (i)–(iii). Fluorescence signals are shown of HSP90 (red) and p239 (green) and merged images (right column) show co-localization of p239 and HSP90 in HepG2 cells (yellow). Bar, 10 μm. (b) Levels of p239 in the cells were examined by immunoblot with p239-specific antibodies, showing decreases of p239 protein with time compared with the β-tubulin control. Levels of proteins were normalized and expressed as a percentage of the homologous protein in the 0 h group.

was close to the surface of cells when HSP90 activity was blocked by GA treatment (Figs 4a, c, upper and middle panels). Pre-treatment with GA also interrupted the translocation, but not the attachment, of p239 (Fig. 4c, upper panels). Therefore, inactivation of HSP90 significantly inhibited the penetration, but not the binding, of p239.

p239 decreases were observed in GA-treated cells (Fig. 4b) and in untreated cells (Fig. 3b). As there was little change

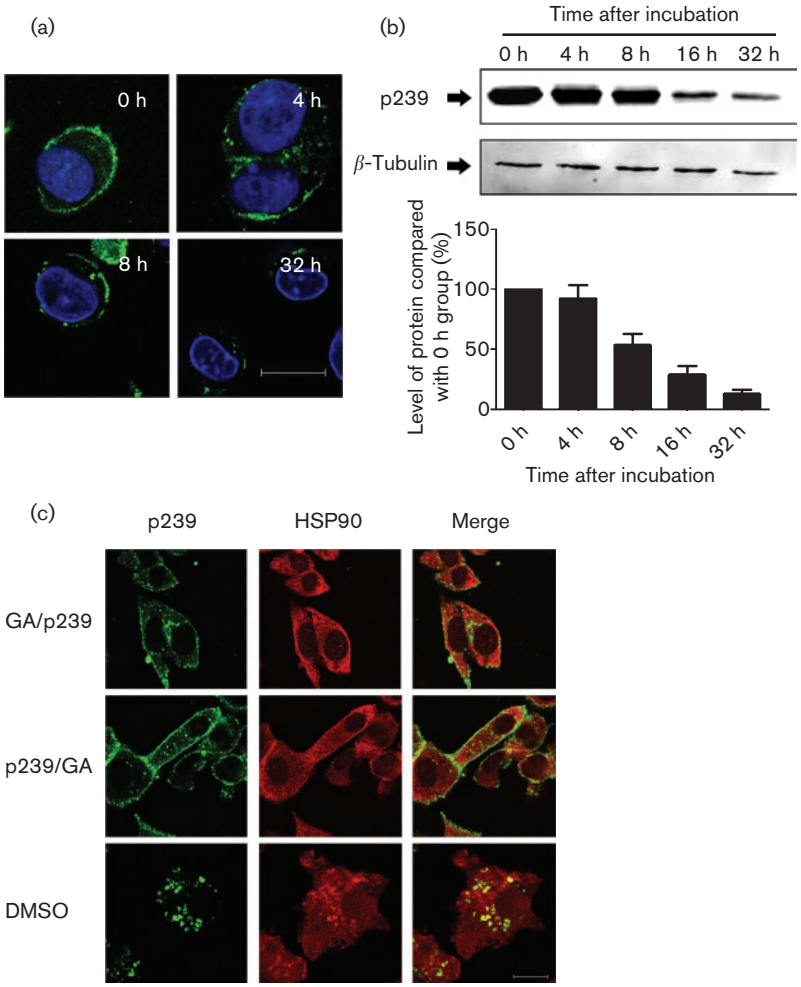

Fig. 4. Inhibition of p239 translocation by HSP90 inhibitor GA. HepG2 cells were incubated with p239 and GA at 4 °C for 30 min, and then recultured for 0, 4, 8, 16 and 32 h at 37 °C. The localization (a) and levels (b) of p239 in the harvested cells were detected and measured. Levels of proteins were normalized and expressed as a percentage of the homologous protein in the 0 h group. (c) HepG2 cells were pre-treated with GA and then incubated with p239 (upper panels) at 4 °C, or cells were incubated with p239 and then treated with GA (middle panels) or with DMSO as a control (lower panels) at 4 °C. After washing and reincubation at 37 °C for 4 h, the cells were stained with antibodies specific for p239 and HSP90. Fluorescence signals are shown of p239 (green) and HSP90 (red) and merged images (right column) show co-localization (yellow). Bar, 10 μm.

between the 0 and 4 h marks shown by Western blot analysis, it was decided to select the 4 h mark as a the time point to note the occurrence or absence of cellular entry.

Immunofluorescence and flow-cytometry techniques were used to detect p239 on the cellular membranes. If the protein was undetected, this would suggest cellular entry. In Fig. 5, p239 was not detected on the surface of cells that had been recultured for 4 h with or without GA. In contrast, it was observed on the cells that were not recultivated. Hence, GA did not affect the membrane crossing of p239. It therefore appears that HSP90 mediates intracellular trafficking, but not surface entry, of p239.

Effect of the HSP90 inhibitor on HEV infectivity

As shown in Fig. 6(a), after 4 h recultivation, strong amplification bands denoting viral RNA were detected in both GA-treated and non-treated cells. However, after 24 h recultivation in cells that were treated with the HSP90 inhibitor, only marginal amounts of viral RNA were detected. Glyceraldehyde-3-phosphate dehydrogenase (G3PDH), used as an internal amplification control, showed no difference. These results suggest that HSP90 is involved in HEV infection. The experiment was repeated with real-time PCR and similar results were obtained (Fig. 6b).

DISCUSSION

In order to replicate, viruses enter the host cell. p239, due to its native-like conformation, antigenicity, immunogenicity and its affinity to binding, was used to simulate HEV. In the present study, p239 was tagged with CBP for fast and easy capture, and for isolation of candidate proteins. Molecular sieve chromatography and cellular binding assay results indicated that the CBP tag had no effect on the characteristics of p239. A group of p239-interacting proteins were isolated and the identified candidates, HSP90 and Grp78/Bip, were examined further by immunoprecipitation and immunofluorescence assays (Figs 2 and 3, and unpublished data) and cultured hepatocytes were infected with wild-type HEV (wtHEV), with results suggesting that p239 is a good experimental surrogate for HEV.

HSP90 is a member of the heat-shock protein family. It is a molecular chaperone that controls the activity,

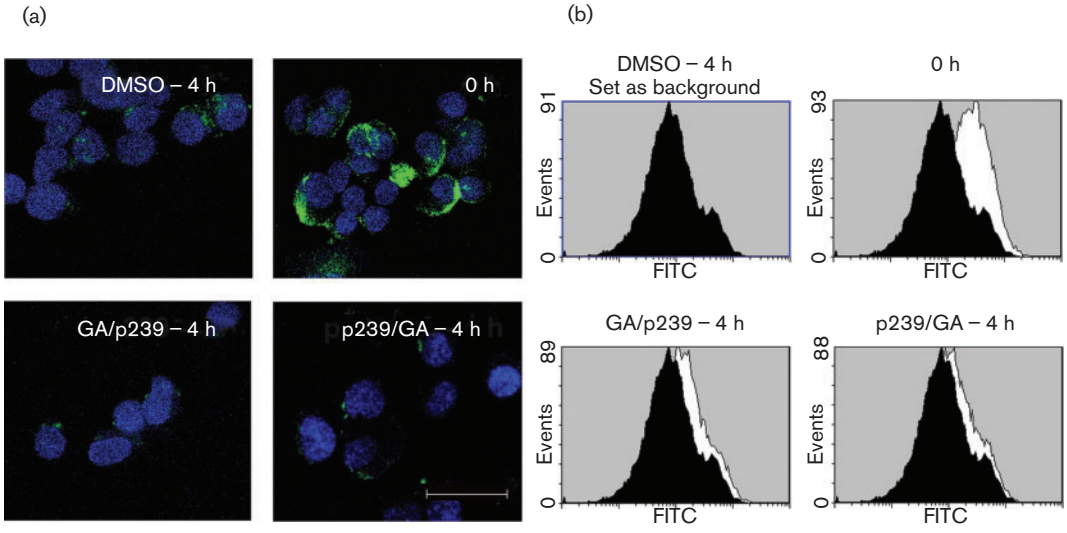

Fig. 5. Cellular membrane crossing of p239 in the presence of the HSP90 inhibitor GA. HepG2 cells were incubated with p239 and then treated with GA (panels 'p239/GA – 4 h') or with DMSO (panels 'DMSO – 4 h') as a control, or cells were pre-treated with GA and then incubated with p239 (panels 'GA/p239 – 4 h') at 4 °C. After washing and reincubation at 37 °C for 4 h, the cells were stained (without being fixed and permeabilized) with p239-specific antibody and FITC-conjugated secondary antibody at 4 °C for 10 min. The cells were then fixed/permeabilized and stained with DAPI and the fluorescence signal was detected using a fluorescence microscope (a) or by flow cytometry (b). Cells incubated with p239 and harvested immediately were used as a positive control for the presence of p239 on the cellular surface (panels '0 h'). Bar, 30 μm.

turnover and trafficking of many proteins (Kumar *et al.*, 2001; Mimnaugh *et al.*, 2006; Thomas *et al.*, 2006). HSP90 is involved in the transportation of the glucocorticoid receptor and glutamine androgen receptor. It works in an ATP- and microtubule-dependent manner to regulate the activity of signalling proteins such as steroid hormone receptors and several kinases (Harrell *et al.*, 2004; Hoffmann & Handschumacher, 1995; Kumar *et al.*, 2001; Mimnaugh *et al.*, 2006; Pratt & Toft, 1997, 2003; Suuronen *et al.*, 2008; Thomas *et al.*, 2006). In addition, the HSP90 trafficking complex has been shown to mediate the import of numerous cellular and viral proteins to the nucleus, playing a critical role in the replication and growth of several viruses. For example, herpes simplex virus type 1 DNA polymerase requires HSP90 for proper localization to the nucleus (Burch & Weller, 2005); it also acts as a stimulatory host factor involved in influenza virus RNA synthesis (Momose *et al.*, 2002). Another study demonstrated that HSP90 is important for vaccinia virus growth in cultured cells through interaction with viral core protein 4a (Hung *et al.*, 2002). HSP90 is required to maintain the function of hepatitis B virus reverse transcriptase (Hu *et al.*, 2004) and the enzyme maturation of hepatitis C virus (Waxman *et al.*, 2001). Recently, HSP90 was also found to be a component of the dengue virus receptor complex in human cells and participated in the entry of the virus (Reyes-Del Valle *et al.*, 2005).

The results from immunofluorescence assays indicated that the behaviour of p239 in hepatocytes can be characterized into three stages: attachment/penetration, cytoplasmic localization and degradation. Additionally, HSP90 was accompanied by p239 in a complex during the entire process (Fig. 2c) and thus it is postulated that HSP90 may be acting in a raft-like role to carry HEV capsids at the cellular membrane and transport them to an appropriate cytoplasmic destination. This hypothesis of the carrier role of HSP90 is enhanced by the results of the GA blocking assay, where the activity of HSP90 was disturbed by GA. A significant proportion of p239 crossed the cellular plasma membrane, but 'adhered' to the cell membrane and did not enter the cytoplasmic region of the cells. In other words, the transportation of p239 from the plasma membrane to an intracellular effective site is mediated by an HSP90-dependent trafficking system.

Interestingly, a recent study shows that highly sulfated heparan sulfate motifs on syndecans are required for binding of HEV ORF2 capsid protein to target cells and HEV infection (Kalia *et al.*, 2009). It suggested that the heparan sulfate proteoglycans may play an attachment receptor role to initiate HEV infection on host cells, while HSP90 undertakes the role of intracellular transportation.

GA, a specific inhibitor of HSP90 function, was compared with three RNA interference (RNAi) constructs to inhibit the function of HSP90. It was found that all RNAi constructs caused cellular injury. Our preliminary results showed that the induction of HSP90 RNAi constructs could inhibit the expression of HSP90 completely and caused a significant cellular injury. Besides its role in the

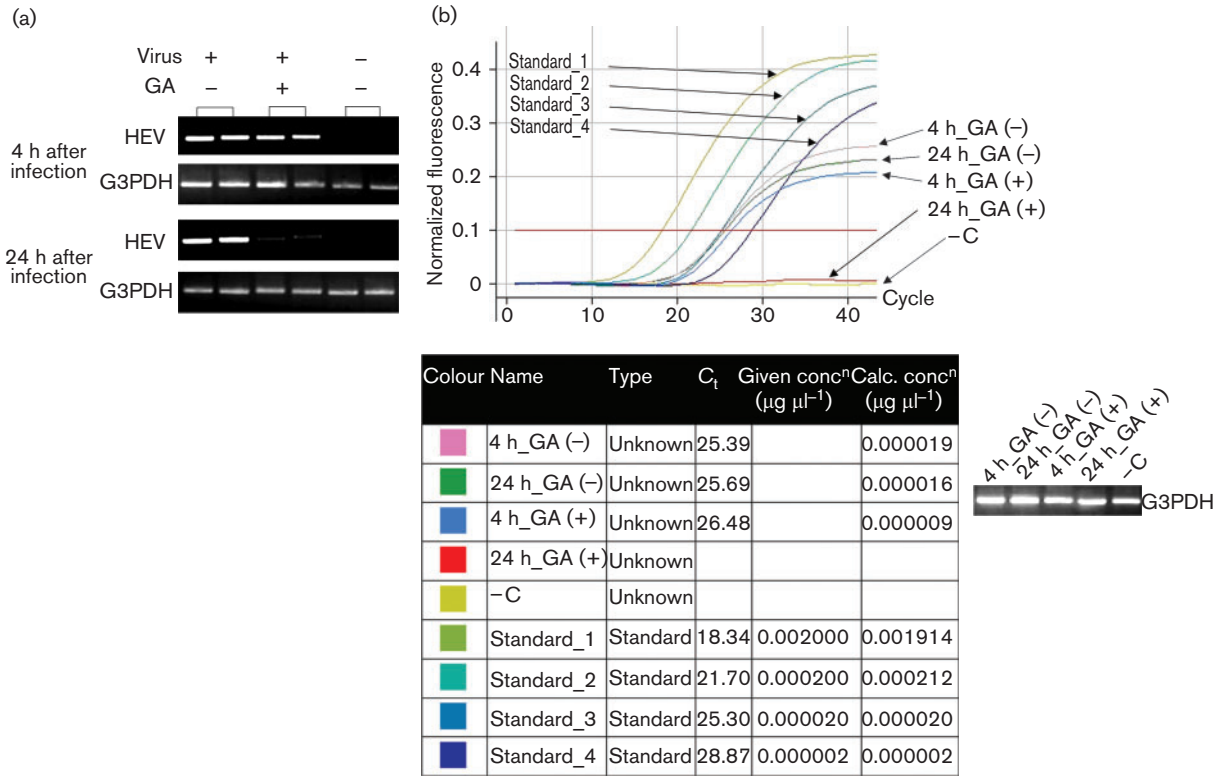

Colour	Name	Type	C_t	Given conc^n (μg μl^{-1})	Calc. conc^n (μg μl^{-1})
	4 h_GA (–)	Unknown	25.39		0.000019
	24 h_GA (–)	Unknown	25.69		0.000016
	4 h_GA (+)	Unknown	26.48		0.000009
	24 h_GA (+)	Unknown			
	–C	Unknown			
	Standard_1	Standard	18.34	0.002000	0.001914
	Standard_2	Standard	21.70	0.000200	0.000212
	Standard_3	Standard	25.30	0.000020	0.000020
	Standard_4	Standard	28.87	0.000002	0.000002

Fig. 6. Inhibition of wtHEV infection by the HSP90 inhibitor GA. (a) HepG2 cells treated with (lanes 3 and 4) or without (lanes 1 and 2) GA were infected with HEV, and then recultured at 37 °C. Viral RNA in the cells was examined at 4 and 24 h after infection. G3PDH RNA in the cells was also examined and used as an internal amplification control. HepG2 cells without HEV infection were used as a negative control (lanes 5 and 6). All of the experiments were carried out in duplicate. (b) The reverse transcriptional samples were also detected by real-time PCR. The threshold cycle (C_t) value and the nucleic acid levels were calculated. The pSK-HEV2 plasmid with gradient dilutions served as standards.

infection process of several viruses, HSP90, as a molecular chaperone, is well-known to be involved in the process of activation, turnover and trafficking of some essential cellular proteins. Therefore, it is no surprise that complete inhibition of HSP90's function will lead to unexpected consequences, e.g. cell-cycle arrest or death. In fact, such kinds of effect by HSP90 small interfering RNA have been reported in a previous study (Kim *et al.*, 2008). Conversely, treatment with GA is much more controllable, taking approximately 30 min at 4 °C before or after incubation of p239/wtHEV in this study, and the function of HSP90 was inhibited in the presence of p239/wtHEV. RNAi constructs are likely to exert effects for over 24 h, whereas GA would exert its effects within 30 min at 4 °C, which was our period of focus. Given these facts, GA was the only viable inhibitor of HSP90.

RT-PCR performed both at 4 and 24 h after inoculation showed no apparent or significant decrease of viral RNA, respectively (Fig. 6). GA treatment affected intracellular movement of the capsids rather than their attachment. As shown in Fig. 4, trafficking of p239 was inhibited by GA, but this was unrelated to reduced amounts of HEV capsid proteins. It is hypothesized that, in GA-treated cells, a reduction in RNA content was due to decreasing viral capsids and that viral RNA intracellular traffic has been influenced by GA.

In conclusion, the HSP90-mediated trafficking system plays an important role in HEV intracellular transportation. Once the virus has become attached to the cell surface, HSP90 assembles at the plasma membrane, the trafficking complex is activated and transportation of HEV from the plasma membrane to the perinuclear sites takes place.

METHODS

Cell lines. HepG2 (HB-8065) cells (obtained from the ATCC) were grown in Dulbecco's modified Eagle's medium containing 10 % fetal calf serum (both from Invitrogen). Antibiotics (100 units ampicillin ml^{-1} and 100 units streptomycin ml^{-1}; HPGC) were added to prevent bacterial contamination at 37 °C in a 5 % CO_2 environment.

Antibodies. HEV capsid protein-specific mAbs were produced in our laboratory. 8C11 and 8H3 are neutralizing antibodies that recognized

conformational determinants, while 15B2 recognized the linear region (He *et al.*, 2008). Rabbit polyclonal antibody (pAb) anti-HSP90, mouse mAb anti-β-tubulin and rabbit pAb anti-α-tubulin were from Santa Cruz Biotechnology. Goat anti-mouse pAb and goat anti-rabbit pAb conjugated with fluorescein isothiocyanate (FITC) or tetramethyl rhodamine isothiocyanate (TRITC) were from Sigma-Aldrich. Goat anti-mouse pAb and goat anti-rabbit pAb conjugated with Alexa Fluor 680 were from Invitrogen.

Viruses. The virus used was isolated from a stool specimen of an acute hepatitis E patient, and was identified as being of genotype 1. A host (a rhesus monkey) was inoculated with the virus; the virus was recovered from a bile sample from the monkey and the titre was determined to be equivalent to 10^7 HEV genome copies by using RT-PCR (Zhang *et al.*, 2003).

Plasmid construction. The p239 sequence and its related information have been described previously (Li *et al.*, 2005). In the present study, the p239 sequence lacking a stop codon was inserted into *Nde*I and *Eco*RI sites of the pTO-T7 expression vector (Xia *et al.*, 2002). CBP (Zheng *et al.*, 1997) was also inserted into the 3′ end of p239 at *Eco*RI and *Hin*dIII sites with the same ORF to generate pTO-T7-p239-CBP. This construct was inserted into bacterial strain Bl-21 (ATCC) and recombinant p239–CBP was expressed and purified.

Protein expression and purification. The plasmid was transformed in *Escherichia coli* ER2566 cells (Invitrogen). The expression and purification of recombinant fusion protein p239–CBP were performed as described previously (Li *et al.*, 2005). In brief, the transformants were cultured in Luria–Bertani medium (Oxoid) with kanamycin overnight, then incubated in the presence of IPTG (both from Amresco) for 6 h. The inclusion bodies were dissolved in 4 M urea (Xilong Chemical) and proteins were renatured by dialysis in PBS, pH 7.45.

Two-site sandwich ELISA. Microtitre plate wells were coated with 100 ng purified 8C11 per well at 37 °C for 3 h, then blocked with PBS containing 20 % bovine serum albumin (Applichem) at 37 °C for 30 min. p239 or p239–CBP was diluted and added to the wells at a concentration of 0, 3.125, 6.25, 12.5, 25, 50, 100, 200 or 400 ng per well and incubated at 37 °C for 30 min. Then, 100 µl of 1 : 1000-diluted horseradish peroxidase-conjugated 8H3 mAbs was added and incubated at 37 °C for 30 min. The wells were washed with PBS with 0.05 % Tween 20 (BBI) and 100 µl tetramethylbenzidine substrate (Sigma Aldrich) was added, and the plates were further incubated for 10 min at 37 °C. The reaction was stopped by adding 50 µl 2 M H_2SO_4 (Xilong Chemical). Absorbance was read at both 450 and 620 nm, with the latter frequency accounting for the background noise.

Gel-filtration HPLC. Purified p239 and p239–CBP were subjected to chromatography through a TSK Gel G5000PWXL 7.8*300 mm column (Tosoh) equilibrated in PBS, pH 7.45, connected to a 126NM/168NM HPLC system equipped with 508 autosampler (Beckman Instruments) to analyse the molecular mass. The column flow rate was maintained at 0.5 ml min^{-1}.

Pull-down assay. A mixture of 0.5 mg p239–CBP proteins and CaM–Sepharose (Amersham Biosciences) in 3 ml CBB buffer [25 mM Tris/HCl (pH 7.5), 150 mM NaCl, 1 mM magnesium acetate, 1 mM imidazole, 2 mM $CaCl_2$, 10 mM β-mercaptoethanol, 0.02 % NP-40] was incubated at 4 °C for 3 h and then washed. The mixture was then incubated in 5 ml HepG2 cell lysis in DDM buffer [20 mM HEPES, 1 mM EGTA (pH 8.0), 5 mM $MgCl_2$, 100 mM NaCl, 10 % glycerol, 0.3 % n-dodecyl β-D-maltoside, protease inhibitors] at 4 °C for 3 h. After three washes with CBB buffer, the proteins associated with CBP-fusion proteins were eluted by 1 ml CEB buffer [25 mM Tris/HCl (pH 7.5), 150 mM NaCl, 1 mM magnesium acetate, 1 mM imidazole, 20 mM EGTA (pH 8.0), 10 mM β-mercaptoethanol, 0.02 % NP-40] and subjected to Western blot assay.

Two-dimensional gel electrophoresis and MALDI-TOF MS. Protein samples were dissolved in IEF buffer [9 M urea, 4 % CHAPS, 2 % IPG buffer, 40 mM dithiothreitol (DTT), 40 mM Tris-base] and loaded into immobilized pH gradient (IPG) strip gels (3-10NL; GE Healthcare). After electrophoresis (30 V 12 h, 200 V 1 h, 500 V 1 h, from 500 to 8000 V 30 min, 8000 V 2 h), IPG strip gels were washed in two buffers [buffer one: 0.05M Tris/HCl (pH 8.8), 6 M urea, 30 % glycerol, 2 % SDS, 65 mM DTT; buffer two: 0.05 M Tris/HCl (pH 8.8), 6 M urea, 30 % glycerol, 2 % SDS, 200 mM iodoacetamide; each buffer for 15 min] and then subjected to electrophoresis in 9 % SDS–polyacrylamide gels. Silver staining was performed at the completion of the experiment (Tunon & Johansson, 1984). For the identification of proteins that interacted with p239, protein spots (analysed by Imagemaster, GE Healthcare) were excised in 1 mm pieces with a razor blade and transferred into discolour buffer (15 mM potassium ferricyanide, 50 mM sodium thiosulfate). The gel was then washed with MilliQ water (Millipore) four times. After shrinking with 100 % acetonitrile (Sigma Aldrich), the gel pieces were rehydrated and digested (Kitatsuji *et al.*, 2007). Less than 1 µl of the sample was spotted onto the MS sample plate (model Reflext MIII; Bruker). The NCBI database was then used to compute the characteristics of the candidate protein.

Isolation and identification of p239-interactive proteins. Silver-stained gels were analysed with Imagemaster software. All candidate protein spots were collected and subjected to tryptic digestion, and the resulting peptide mixtures were analysed by MALDI-TOF MS according to the manufacturer's instructions. The peptide maps were compared with the Mass Spectrometry protein sequence Database (MSDB) using Mascot software (http://www.matrixscience.com).

Immunoprecipitation. Cell extracts from HepG2 cells (pre-incubated with p239 for 4 h) were incubated with antibodies against HSP90 or p239 or with a control rabbit pAb against the haemagglutinin (HA) tag at 4 °C for 3 h in lysis buffer [20 mM KOH-HEPES (pH 8.0), 0.2 mM EDTA, 5 % glycerol, 250 mM NaCl, 0.5 % NP-40, 0.25 % sodium deoxycholate, 1 mM DTT and protease inhibitors), and the immune complexes were collected by incubation with 30 µl protein A/G PLUS-Agarose (Santa Cruz Biotechnology) for 2 h. Immunoprecipitates were washed three times with lysis buffer supplemented with NaCl to 400 mM and then a Western blot assay was performed.

Immunoblot. The cells were harvested by cell lysis [20 mM KOH-HEPES (pH 8.0), 0.2 mM EDTA, 5 % glycerol, 250 mM NaCl, 0.5 % NP-40, 0.25 % sodium deoxycholate, 1 mM DTT and protease inhibitors], and then the samples were separated by SDS-PAGE and transferred onto a nitrocellulose membrane (Whatman). After transfer, the membrane was immersed for 30 min in blocking solution (5 % non-fat milk in PBS, pH 7.45) and washed in PBS containing 0.1 % Tween 20. Then, the membrane was incubated with primary antibody and washed a further three times with 0.1 % PBS-Tween. Alexa Fluor 680-conjugated pAbs as the secondary antibody were then added and the reaction signals were examined by Odessey (Li-COR).

Immunofluorescence. HepG2 cells cultured on coverslips were incubated with and without p239 and treated with and without GA in the experimental matrix shown in Table 1.

The cells were fixed with 4 % paraformaldehyde (Sigma Aldrich) and permeabilized with 0.1 % Triton (Amresco) in PBS. The samples were

Table 1. Experimental matrix used for immunofluorescence

	With p239	Without p239
With GA	Experiment conducted	Not done
Without GA	Experiment conducted	Experiment conducted

blocked with 10 % goat serum in PBS for 15 min, incubated with a mixture of 15B2 (anti-p239 mouse mAb) and anti-HSP90 rabbit pAb for 30 min, and then labelled by FITC- or TRITC-conjugated secondary antibodies for 30 min. After being washed three times, the cells were stained with 0.5 % 4′,6-diamidino-2-phenylindole (DAPI; Invitrogen). The fluorescence signals were detected with a laser-scanning confocal microscope (Leica).

Flow cytometry. HepG2 cells pre-incubated with p239 were treated with or without GA and then were harvested immediately or after recultivation. The samples were incubated with a mixture of 15B2 (anti-p239 mouse mAb) and FITC-conjugated secondary antibodies for 15 min at 4 °C. After being washed three times at 4 °C in PBS, the presence of p239 was detected by flow cytometry (Beckman Coulter Epics XL).

RT-PCR. The presence of HEV RNA in cells was detected by RT-PCR. The RT-PCR protocols and primers used for the detection of genotype 1 HEV have been described previously (Zhang *et al.*, 2005). G3PDH RNA was used as an internal amplification control.

Real-time PCR. Using PCR protocols and primers described previously (Jothikumar *et al.*, 2006), a 2 μm reverse transcription sample was detected by real-time PCR. The fluorescence signal generated was measured by Rotor-Gene RG-3000 (Corbett Research) and analysed using the Rotor Gene 6 software. The pSK-HEV2 plasmid, obtained from Dr Suzanne U. Emerson (Graff *et al.*, 2008), was diluted to a concentration between 2×10^{-3} and 2×10^{-6} μg μl^{-1} and the diluted plasmids were served as standard samples. The threshold fluorescence level was set automatically by the software. The threshold cycle (C_t) value and nucleic acid level were determined automatically for each sample. G3PDH RNA detected by RT-PCR was used as a control of RNA loading.

Use of GA. GA has been reported as an inhibitor of HSP90 and is used widely in HSP90 research (Hu & Seeger, 1996). It is known that GA binds to a conserved binding pocket in the N-terminal domain of HSP90, inhibits ATP binding, and consequently blocks ATP-dependent HSP90 chaperone activity (Hu & Seeger, 1996). In order to explore further the role of HSP90 on p239 translocation, HepG2 cells were incubated with p239 for 30 min at 4 °C, then with 10 μM GA (dissolved within DMSO; both from Sigma Aldrich) or with DMSO as a vehicle control for additional 30 min at 4 °C, or cells were pre-treated with 10 μM GA for 30 min, then incubated with p239 for additional 30 min at 4 °C. Reincubation was for 4 h at 37 °C, and p239 and HSP90 were stained and observed.

Detection of extracellular p239. Cells treated and incubated as mentioned above were isolated by trypsin digestion and then stained directly with p239-specific antibody and FITC-conjugated secondary antibody at 4 °C for 10 min. The cells were then fixed with 4 % paraformaldehyde, and permeabilized in 0.1 % Triton in PBS and stained with 0.5 % DAPI. The fluorescence signal was detected with fluorescence microscopy or flow cytometry.

Infectivity protocol. Previous findings indicate that HEV has a limited ability to infect and replicate in HepG2 cells (Emerson *et al.*, 2005, 2006; He *et al.*, 2008). In blocking experiments, HepG2 cells were initially treated with HEV for 1 h at 4 °C. Then, the cells were incubated with 10 μM GA (dissolved within DMSO) or DMSO as vehicle control for 30 min at 4 °C, followed by 4 or 24 h incubation at 37 °C. Cells that lack HEV infection and GA treatment were used as controls. After incubation, cells were harvested immediately and RNA extracted.

ACKNOWLEDGEMENTS

This work was supported in part by research of grants from the Ministry of Education of China (30870514, 30600106 and 30500092), the Ministry of Science and Technology of China (2006AA02A209) and Fujian Province, China (2006F3124). We thank Dr Suzanne U. Emerson (Laboratory of Infectious Diseases, National Institutes of Health, Bethesda, MD, USA) for proving plasmid pSK-HEV2. We would also like to thank Dr Munhon Ng and Dr James W. K. Shih for their assistance in writing this manuscript.

REFERENCES

Bradley, D., Andjaparidze, A., Cook, E. H., Jr, McCaustland, K., Balayan, M., Stetler, H., Velazquez, O., Robertson, B., Humphrey, C. & other authors (1988). Aetiological agent of enterically transmitted non-A, non-B hepatitis. *J Gen Virol* **69**, 731–738.

Burch, A. D. & Weller, S. K. (2005). Herpes simplex virus type 1 DNA polymerase requires the mammalian chaperone hsp90 for proper localization to the nucleus. *J Virol* **79**, 10740–10749.

Emerson, S. U., Nguyen, H., Graff, J., Stephany, D. A., Brockington, A. & Purcell, R. H. (2004). *In vitro* replication of hepatitis E virus (HEV) genomes and of an HEV replicon expressing green fluorescent protein. *J Virol* **78**, 4838–4846.

Emerson, S. U., Arankalle, V. A. & Purcell, R. H. (2005). Thermal stability of hepatitis E virus. *J Infect Dis* **192**, 930–933.

Emerson, S. U., Clemente-Casares, P., Moiduddin, N., Arankalle, V. A., Torian, U. & Purcell, R. H. (2006). Putative neutralization epitopes and broad cross-genotype neutralization of hepatitis E virus confirmed by a quantitative cell-culture assay. *J Gen Virol* **87**, 697–704.

Graff, J., Torian, U., Nguyen, H. & Emerson, S. U. (2006). A bicistronic subgenomic mRNA encodes both the ORF2 and ORF3 proteins of hepatitis E virus. *J Virol* **80**, 5919–5926.

Graff, J., Zhou, Y. H., Torian, U., Nguyen, H., St Claire, M., Yu, C., Purcell, R. H. & Emerson, S. U. (2008). Mutations within potential glycosylation sites in the capsid protein of hepatitis E virus prevent the formation of infectious virus particles. *J Virol* **82**, 1185–1194.

Guu, T. S., Liu, Z., Ye, Q., Mata, D. A., Li, K., Yin, C., Zhang, J. & Tao, Y. J. (2009). Structure of the hepatitis E virus-like particle suggests mechanisms for virus assembly and receptor binding. *Proc Natl Acad Sci U S A* **106**, 12992–12997.

Harrell, J. M., Murphy, P. J., Morishima, Y., Chen, H., Mansfield, J. F., Galigniana, M. D. & Pratt, W. B. (2004). Evidence for glucocorticoid receptor transport on microtubules by dynein. *J Biol Chem* **279**, 54647–54654.

He, S., Miao, J., Zheng, Z., Wu, T., Xie, M., Tang, M., Zhang, J., Ng, M. H. & Xia, N. (2008). Putative receptor-binding sites of hepatitis E virus. *J Gen Virol* **89**, 245–249.

Hoffmann, K. & Handschumacher, R. E. (1995). Cyclophilin-40: evidence for a dimeric complex with hsp90. *Biochem J* **307**, 5–8.

Hu, J. & Seeger, C. (1996). Hsp90 is required for the activity of a hepatitis B virus reverse transcriptase. *Proc Natl Acad Sci U S A* **93**, 1060–1064.

Hu, J., Flores, D., Toft, D., Wang, X. & Nguyen, D. (2004). Requirement of heat shock protein 90 for human hepatitis B virus reverse transcriptase function. *J Virol* **78**, 13122–13131.

Huang, R., Nakazono, N., Ishii, K., Li, D., Kawamata, O., Kawaguchi, R. & Tsukada, Y. (1995). Hepatitis E virus (87A strain) propagated in A549 cells. *J Med Virol* **47**, 299–302.

Huang, Y. W., Opriessnig, T., Halbur, P. G. & Meng, X. J. (2007). Initiation at the third in-frame AUG codon of open reading frame 3 of the hepatitis E virus is essential for viral infectivity *in vivo*. *J Virol* **81**, 3018–3026.

Hung, J. J., Chung, C. S. & Chang, W. (2002). Molecular chaperone Hsp90 is important for vaccinia virus growth in cells. *J Virol* **76**, 1379–1390.

Jothikumar, N., Cromeans, T. L., Robertson, B. H., Meng, X. J. & Hill, V. R. (2006). A broadly reactive one-step real-time RT-PCR assay for rapid and sensitive detection of hepatitis E virus. *J Virol Methods* **131**, 65–71.

Kalia, M., Chandra, V., Rahman, S. A., Sehgal, D. & Jameel, S. (2009). Heparan sulfate proteoglycans are required for cellular binding of the hepatitis E virus ORF2 capsid protein and for viral infection. *J Virol* **83**, 12714–12724.

Kim, Y. H., Kim, Y. S., Park, C. H., Chung, I. Y., Yoo, J. M., Kim, J. G., Lee, B. J., Kang, S. S., Cho, G. J. & other authors (2008). Protein kinase C-delta mediates neuronal apoptosis in the retinas of diabetic rats via the Akt signaling pathway. *Diabetes* **57**, 2181–2190.

Kitatsuji, C., Kurogochi, M., Nishimura, S., Ishimori, K. & Wakasugi, K. (2007). Molecular basis of guanine nucleotide dissociation inhibitor activity of human neuroglobin by chemical cross-linking and mass spectrometry. *J Mol Biol* **368**, 150–160.

Kumar, R., Grammatikakis, N. & Chinkers, M. (2001). Regulation of the atrial natriuretic peptide receptor by heat shock protein 90 complexes. *J Biol Chem* **276**, 11371–11375.

Li, S. W., Zhang, J., Li, Y. M., Ou, S. H., Huang, G. Y., He, Z. Q., Ge, S. X., Xian, Y. L., Pang, S. Q. & other authors (2005). A bacterially expressed particulate hepatitis E vaccine: antigenicity, immunogenicity and protectivity on primates. *Vaccine* **23**, 2893–2901.

Li, S., Tang, X., Seetharaman, J., Yang, C., Gu, Y., Zhang, J., Du, H., Shih, J. W., Hew, C. L. & other authors (2009). Dimerization of hepatitis E virus capsid protein E2s domain is essential for virus-host interaction. *PLoS Pathog* **5**, e1000537.

Meng, J., Dubreuil, P. & Pillot, J. (1997). A new PCR-based seroneutralization assay in cell culture for diagnosis of hepatitis E. *J Clin Microbiol* **35**, 1373–1377.

Meng, J., Dai, X., Chang, J. C., Lopareva, E., Pillot, J., Fields, H. A. & Khudyakov, Y. E. (2001). Identification and characterization of the neutralization epitope(s) of the hepatitis E virus. *Virology* **288**, 203–211.

Mimnaugh, E. G., Xu, W., Vos, M., Yuan, X. & Neckers, L. (2006). Endoplasmic reticulum vacuolization and valosin-containing protein relocalization result from simultaneous hsp90 inhibition by geldanamycin and proteasome inhibition by velcade. *Mol Cancer Res* **4**, 667–681.

Momose, F., Naito, T., Yano, K., Sugimoto, S., Morikawa, Y. & Nagata, K. (2002). Identification of Hsp90 as a stimulatory host factor involved in influenza virus RNA synthesis. *J Biol Chem* **277**, 45306–45314.

Pratt, W. B. & Toft, D. O. (1997). Steroid receptor interactions with heat shock protein and immunophilin chaperones. *Endocr Rev* **18**, 306–360.

Pratt, W. B. & Toft, D. O. (2003). Regulation of signaling protein function and trafficking by the hsp90/hsp70-based chaperone machinery. *Exp Biol Med (Maywood)* **228**, 111–133.

Reyes-Del Valle, J., Chavez-Salinas, S., Medina, F. & Del Angel, R. M. (2005). Heat shock protein 90 and heat shock protein 70 are components of dengue virus receptor complex in human cells. *J Virol* **79**, 4557–4567.

Suuronen, T., Ojala, J., Hyttinen, J. M., Kaarniranta, K., Thornell, A., Kyrylenko, S. & Salminen, A. (2008). Regulation of ER alpha signaling pathway in neuronal HN10 cells: role of protein acetylation and Hsp90. *Neurochem Res* **33**, 1768–1775.

Tanaka, T., Takahashi, M., Kusano, E. & Okamoto, H. (2007). Development and evaluation of an efficient cell-culture system for hepatitis E virus. *J Gen Virol* **88**, 903–911.

Thomas, M., Harrell, J. M., Morishima, Y., Peng, H. M., Pratt, W. B. & Lieberman, A. P. (2006). Pharmacologic and genetic inhibition of hsp90-dependent trafficking reduces aggregation and promotes degradation of the expanded glutamine androgen receptor without stress protein induction. *Hum Mol Genet* **15**, 1876–1883.

Tunon, P. & Johansson, K. E. (1984). Yet another improved silver staining method for the detection of proteins in polyacrylamide gels. *J Biochem Biophys Methods* **9**, 171–179.

Waxman, L., Whitney, M., Pollok, B. A., Kuo, L. C. & Darke, P. L. (2001). Host cell factor requirement for hepatitis C virus enzyme maturation. *Proc Natl Acad Sci U S A* **98**, 13931–13935.

Xia, N. S., Luo, W. X., Zhang, J., Xie, X. Y., Yang, H. J., Li, S. W., Chen, M. & Ng, M. H. (2002). Bioluminescence of *Aequorea macrodactyla*, a common jellyfish species in the East China Sea. *Mar Biotechnol (NY)* **4**, 155–162.

Yamashita, T., Mori, Y., Miyazaki, N., Cheng, R. H., Yoshimura, M., Unno, H., Shima, R., Moriishi, K., Tsukihara, T. & other authors (2009). Biological and immunological characteristics of hepatitis E virus-like particles based on the crystal structure. *Proc Natl Acad Sci U S A* **106**, 12986–12991.

Zhang, J., Ge, S. X., Huang, G. Y., Li, S. W., He, Z. Q., Wang, Y. B., Zheng, Y. J., Gu, Y., Ng, M. H. & other authors (2003). Evaluation of antibody-based and nucleic acid-based assays for diagnosis of hepatitis E virus infection in a rhesus monkey model. *J Med Virol* **71**, 518–526.

Zhang, J., Gu, Y., Ge, S. X., Li, S. W., He, Z. Q., Huang, G. Y., Zhuang, H., Ng, M. H. & Xia, N. S. (2005). Analysis of hepatitis E virus neutralization sites using monoclonal antibodies directed against a virus capsid protein. *Vaccine* **23**, 2881–2892.

Zheng, C. F., Simcox, T., Xu, L. & Vaillancourt, P. (1997). A new expression vector for high level protein production, one step purification and direct isotopic labeling of calmodulin-binding peptide fusion proteins. *Gene* **186**, 55–60.